Proc. SPIE preprint 7736-34, San Diego (2010)

Characterization of OCam and CCD220, the fastest and most sensitive camera to date for AO wavefront sensing

Philippe Feautrier[a1], Jean-Luc Gach[b], Philippe Balard[b], Christian Guillaume[c], Mark Downing[d], Norbert Hubin[d], Eric Stadler[a], Yves Magnard[a], Michael Skegg[e], Mark Robbins[e], Sandy Denney[e], Wolfgang Suske[e], Paul Jorden[e], Patrick Wheeler[e], Peter Pool[e], Ray Bell[e], David Burt[e], Ian Davies[e], Javier Reyes[d], Manfred Meyer[d], Dietrich Baade[d], Markus Kasper[d], Robin Arsenault[d], Thierry Fusco[f] and José Javier Diaz Garcia[g]

[a]LAOG, Domaine Universitaire, 414 rue de la Piscine, BP 53 38041 Grenoble Cedex 9, France;
[b]LAM, Laboratoire d'Astrophysique de Marseille, Technopôle de Château-Gombert - 38, rue Frédéric Joliot-Curie -13388 Marseille, France;
[c]OHP, Observatoire de Haute Provence, 04870 St.Michel l'Observatoire, France;
[d]ESO, Karl-Schwarzschild-Strasse 2, 85748 Garching bei München, Germany;
[e]e2v technologies,106 Waterhouse Lane, Chelmsford, Essex, CM1 2QU, England;
[f]ONERA, BP 72, 92322 Chatillon Cedex, France;
[g]IAC, Instituto de Astrofisica de Canarias, 38200 La Laguna, Islas Canarias, Spain.

ABSTRACT

For the first time, sub-electron read noise has been achieved with a camera suitable for astronomical wavefront-sensing (WFS) applications. The OCam system has demonstrated this performance at 1300 Hz frame rate and with 240x240-pixel frame rate.

ESO and JRA2 OPTICON[2] have jointly funded e2v technologies to develop a custom CCD for Adaptive Optics (AO) wavefront sensing applications. The device, called CCD220, is a compact Peltier-cooled 240x240 pixel frame-transfer 8-output back-illuminated sensor using the EMCCD technology. This paper demonstrates sub-electron read noise at frame rates from 25 Hz to 1300 Hz and dark current lower than 0.01 e-/pixel/frame. It reports on the comprehensive, quantitative performance characterization of OCam and the CCD220 such as readout noise, dark current, multiplication gain, quantum efficiency, charge transfer efficiency... OCam includes a low noise preamplifier stage, a digital board to generate the clocks and a microcontroller. The data acquisition system includes a user friendly timer file editor to generate any type of clocking scheme. A second version of OCam, called OCam^2, was designed offering enhanced performances, a completely sealed camera package and an additional Peltier stage to facilitate operation on a telescope or environmentally rugged applications. OCam^2 offers two types of built-in data link to the Real Time Computer: the CameraLink industry standard interface and various fiber link options like the sFPDP interface. OCam^2 includes also a modified mechanical design to ease the integration of microlens arrays for use of this camera in all types of wavefront sensing AO system. The front cover of OCam^2 can be customized to include a microlens exchange mechanism.

Keywords: Adaptive optics, AO systems, Electron Multiplying CCD, EMCCD, L3Vision CCD, low readout noise, wavefront sensor, sub-electron noise.

1. INTRODUCTION

The success of the next generation of ESO (European Southern Observatory) instruments [1] for 8 to 10-m class telescopes will depend on the ability of Adaptive Optics (AO) systems to provide excellent image quality and stability. This will be achieved by increasing the sampling and correction of the wave front error in both spatial and time domains. For example, advanced Shack Hartmann systems currently fabricated require 40x40 sub-apertures at sampling rates of 1-

[1] Contact address: philippe.feautrier@obs.ujf-grenoble.fr
[2] OPTICON EU Sixth Framework Programme contract number is RII3-CT-2004-001566.

1.5 kHz as opposed to 14x14 sub-apertures at 500 Hz of previous AO systems. Detectors of 240x240 pixels will be required to provide the spatial dynamics of 5-6 pixels per sub-aperture. Higher temporal-spatial sampling implies fewer photons per pixel therefore the need for much lower read noise (<<1e-) and negligible dark current (<< 1e-/pixel/frame) to detect and centroid on a small number of photons

The detector development described in this paper was jointly funded by ESO and the OPTICON European network [2] in the Joint Research Activity JRA2 [3], "Fast Detectors for Adaptive Optic". *e2v technologies*[3] was chosen in 2005 to develop a dedicated detector based on an extension of their L3Vision [4] EMCCD technology. Analysis [5] showed that the sub-electron read noise of L3Vision CCDs clearly outperformed classical CCDs even though L3Vision devices exhibit the excess noise factor F of $2^{1/2}$ typical of EMCCDs [6]. The reason for this conclusion is clearly shown in the results (see Figure 1) of an analysis [7] for the ESO instrument SPHERE [8] for two different types of natural guide stars (GS), white-yellow and red, where a much higher Strehl Ratio is achieved for a faint guide star by an EMCCD than a classical CCD even though it was assumed that the classical CCD had a much higher quantum efficiency in the red. See some example of OCam integration in SPHERE AO system in the Figure 2.

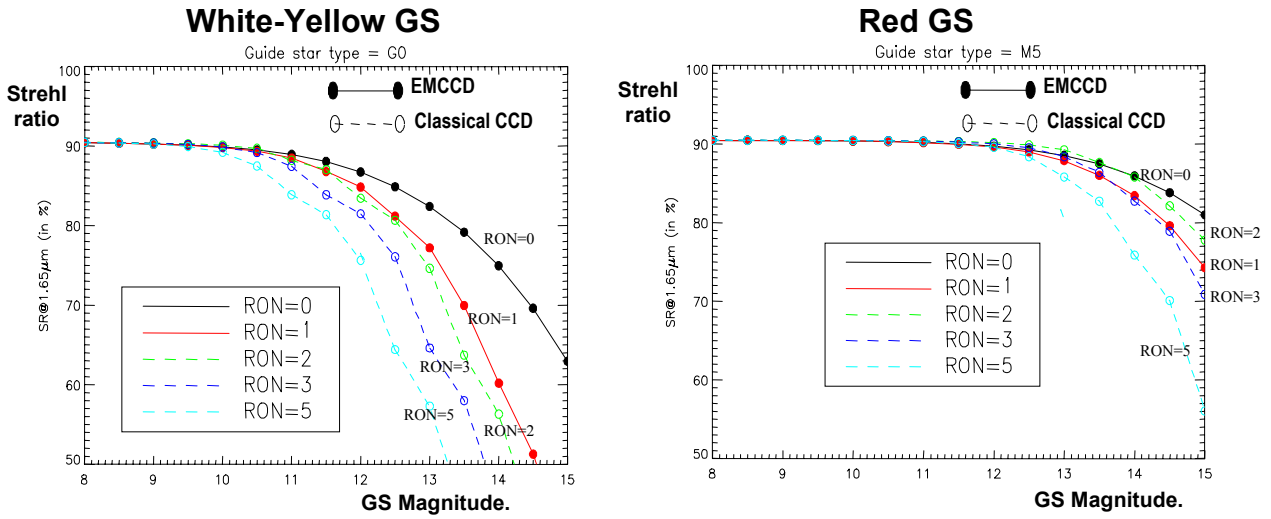

Figure 1. Results of analysis performed for ESO instrument SPHERE[5] that compares an EMCCD of read out noise (RON) 0 and 1e- to a classical CCD of read noise 2, 3, and 5e- for two different types of guide stars. Left: Plots of Strehl Ratio versus GS magnitude for white-yellow guide star. Right: Plots of Strehl Ratio versus GS magnitude for red guide star.

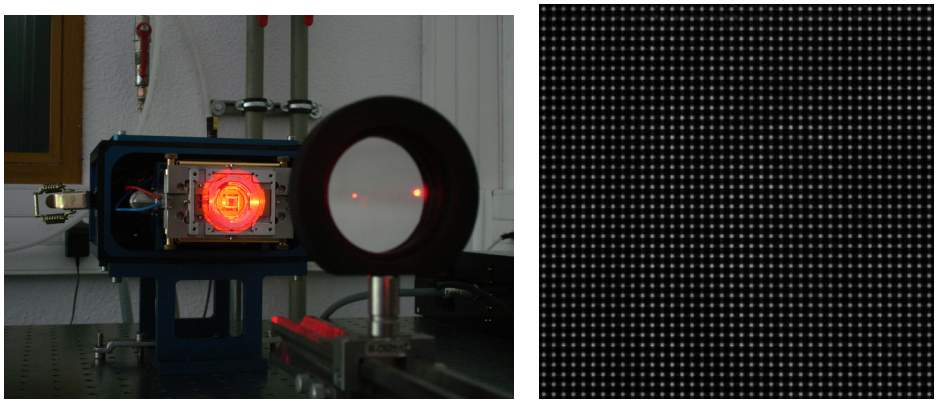

Figure 2: 40x40 microlens array integration on OCam prototype for SPHERE [5] AO loop testing. Left: test setup for microlens alignment and integration. Right: image of the 40x40 lenslet array on OCam.

The roadmap of ESO's WFS detector development program is presented in another paper of this conference [9].

[3] e2v technologies, http://www.e2v.com/.

2. THE CCD220 DESIGN

The CCD220 was the name chosen by *e2v technologies* for this detector. The CCD220 [9], [10], [11], [12], [13] (schematic in Figure 3) is a 24 µm square 240x240 pixels split frame transfer back illuminated L3Vision CCD. The image and store area (store is optically shielded) are built with 2-phase metal-buttressed parallel clock structures to enable fast line shifts in excess of 7 Mlines/s for total transfer time from image to store of 18 µs and low smearing of under 2% at 1200 fps. Eight Electron-Multiplying [4] registers operating at greater than 13 Mpixel/sec enable sub electron noise to be achieved at frame rates of 1300 fps.

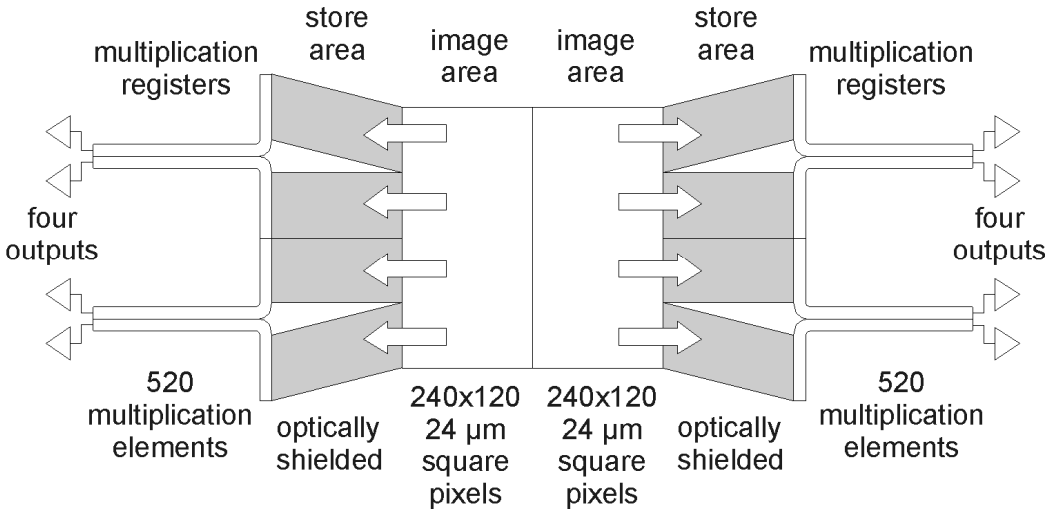

Figure 3: Schematic of e2v technologies 240x240 pixel L3Vision CCD220. Eight Electron-Multiplying (gain) registers are used to obtain sub-electron noise at frame rates of 1300 fps.

The CCD220 is encapsulated in a 64 pin package (see Figure 4) with a custom-designed integral Peltier cooler that cools down the CCD below -45°C to achieve the required total dark current. The package is sealed and back-filled with 0.9 bar of Krypton gas to minimize heat transfer to the outside. Extensive thermal modeling [14] of the CCD, Peltier cooler, package, proposed clamping arrangement and water-cooled heat exchanger was performed. The modeling results which have been verified by measurement show that for 10 °C water temperature in the heat exchanger, the Peltier can cool the CCD to below -45 °C. This enables the dark current specification (<0.01 e/pix/frame at 1300 fps and <0.04 e/pix/frame at 25 fps) of the standard silicon device to be easily achieved.

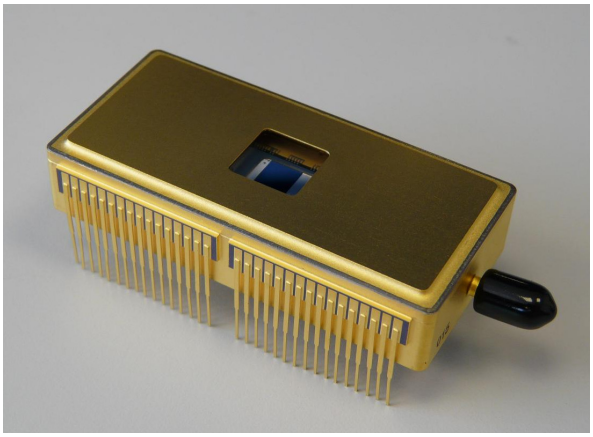

Figure 4. Photograph of CCD220 package with integral Peltier cooler that has been verified (first by thermal modeling then by measurement) to cool the CCD below -45°C to achieve < 0.01 e-/pix/frame total dark current.

3. THE OCam CONTROLLER

3.1 The OCAM controller presentation

The OCAM camera has been designed to test and operate the CCD220. The analog electronics of OCam also forms a critical part of the adaptive-optics branch of ESO's NGC controller [9], [15].

The controller is divided into four parts that are shown in Figure 5: an acquisition system, an interface board, the internal microcontroller that manages the drive electronics and the link to the data acquisition system controller.

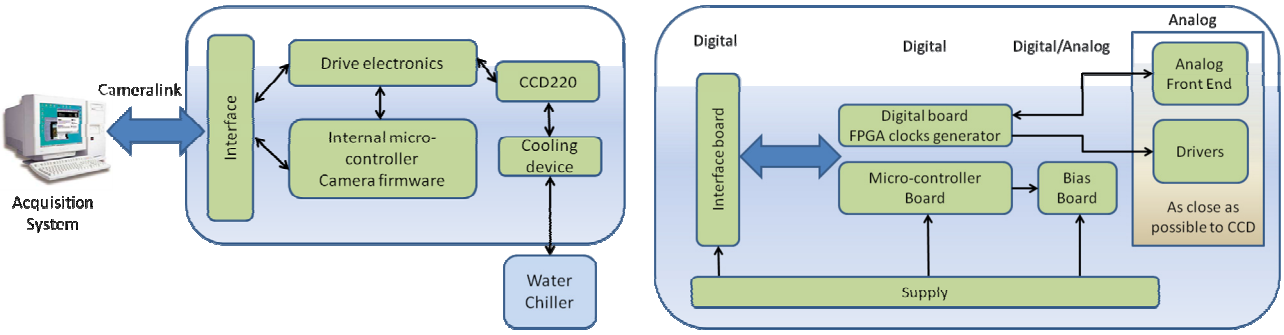

Figure 5. OCam controller block diagram. Left: OCam controller global architecture; Right: OCam controller design with detailed breakdown structure of the electronic boards.

The design was carefully optimized for ultra low noise operation. Particular care was taken to minimize Radio-Frequency perturbations. The drive electronics was designed to be as close as possible to the CCD in order to minimize parasitic inductance (from tracks/pins) and enable high parallel clocking frequencies (see Figure 6). Only a few centimeters separate the CCD die from the video preamplifiers with the OCam design.

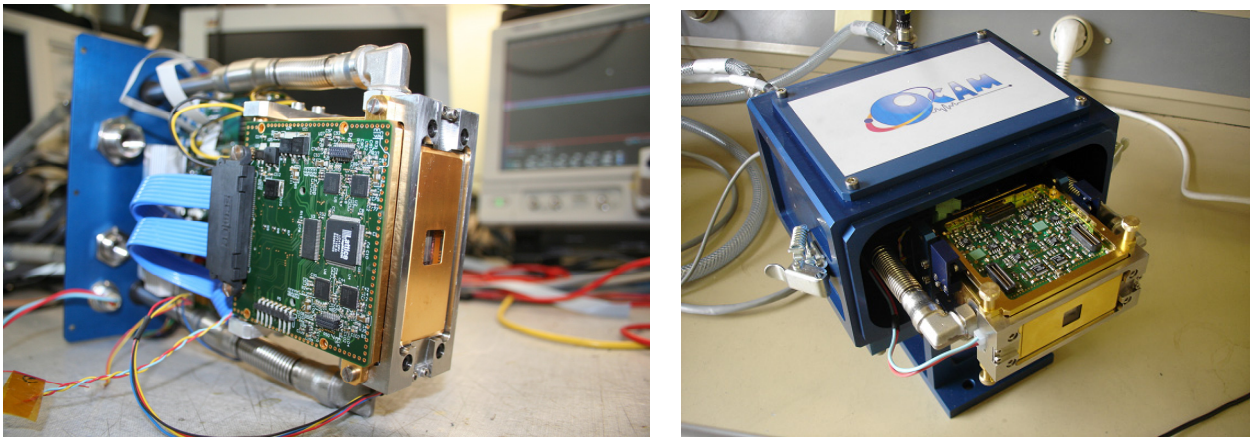

Figure 6. OCam controller views showing the front end electronics as close as possible to the CCD220.

3.2 Main OCAM controller characteristics

The OCam system is capable of driving all members of the CCD220/219 family at their nominal speed (1.5kframes/s) and transmitting the data at full speed through a CameraLink interface. The camera controller is able to drive deep depleted variants with multilevel clocking at voltage levels up to 24V with speeds of 10Mlines/s (at a nominal phase load of 1nF). To obtain such a speed, OCam uses a special phase generation scheme. an arbitrary waveform generator is used. The core sequencer feeds a fast 14bit D/A converter running at 109 Mfps followed by a class AB power amplifier that drives the CCD's phase. Using this generation method, it is possible to compensate for the parasitic PCB track/package pin inductance that makes a resonator with the CCD's phase and produce potentially destructive overshoots by using de-

emphasis and suitable drive waveforms. This method can also be used to reduce the slew rate of the phase drive in order to minimize the generated Clock Induced Charges (CIC) [16] .

The controller handles the 8 L3vision outputs with high voltage clocking up to 50V voltage swing. A big effort has been made to have high voltage stability (less that 1mV/hour of drift) in order to ensure a constant gain over a long period. The system digitizes the CCD signal using correlated double sampling with 14 bits resolution. Standard interfacing of the camera is performed by using a PC computer running Windows OS fitted with a CameraLink full grabber and a proprietary software capable of gathering in real time the extremely high data rate of 220Mbytes/s produced by the camera.

In addition, the team developed a user-friendly timer file editor to manage the clock sequencer of OCam. The sequencer itself is the heart of the system; it has a nominal resolution of 1.5ns and is capable of generating clocks at a frequency of 327MHz. The phase jitter was measured at a level of 60ps RMS.

4. OCam AND CCD220 PERFORMANCES

The calibration and performance measurement of OCam and the CCD220 requires non-standard techniques due to the extreme performances of this system. The main calibration methods are described in this section including measured performance.

4.1 System gain calibration

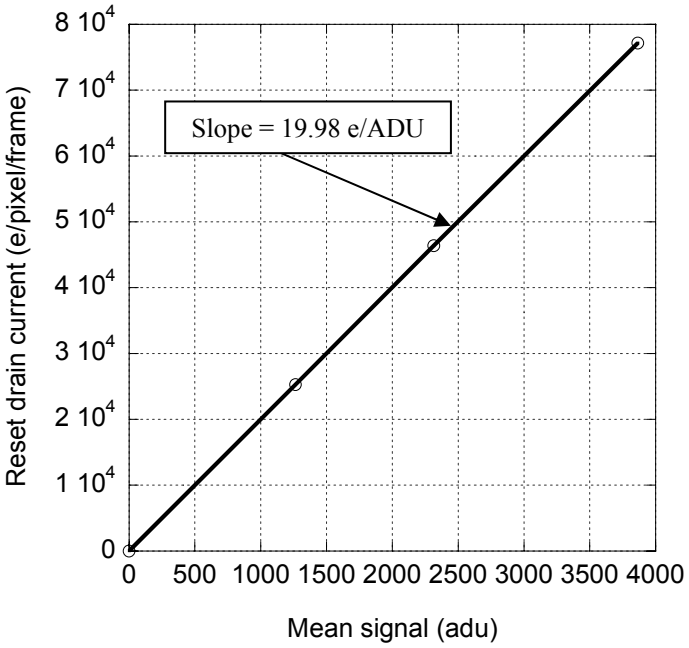

Figure 7: Evaluation of the camera average system gain using direct measurement of the reset drain current.

Camera calibrations usually rely on the photon-transfer curve which plots the signal variance as a function of the signal level. At medium signal level, a digital camera is normally shot noise limited as this exceeds the readout noise floor. The shot noise is characterized by the fact that its RMS value is equal to the square root of the mean number of photons incident on a given pixel. Thus, the shot noise curve becomes a straight line when the variance is plotted as a function of the mean signal and the inverse slope of this linear curve give the system gain in e/ADU [17]. This supposes that all other sources of noise are not significant in the acquired data, such as readout noise, PRNU noise (Photon Response Non Uniformity) or system correlated noise. The shot noise has nothing to do with the camera noise and is only due to the nature of light. For this calibration, any mean/variance measurement must be performed without multiplication gain to avoid influence of the excess noise factor from EMCCD devices.

With OCam, we observed that the photon transfer curve was inappropriate because of correlated noise sources in our system. Finally, the system gain was computed by using the direct measurement of the reset drain current of the whole 240x240 pixels image. The reset drain current is measured with an ammeter imbedded inside OCam which measures the total current of each frame with an accuracy of 10 pA. The reset current measured by OCam is simply divided by the frame rate, the number of pixels (240^2) and the charge of the electron to obtain the reset current in e/pixel/frame. Knowing the reset current in e/pixel/frame and the mean signal (in ADU) allows to plot a calibration curve similar to that of Figure 7. This plot is linear, the slope of the linear regression is directly the mean system gain in e/ADU. This method has the advantage of being valid in any case, but the drawback is that the system gain is averaged over the whole frame and cannot be computed separately for each output. A careful calibration of the OCam analog chain gain gives good confidence in the calibration, resulting in a constant system gain over the 8 channels of the CCD.

4.2 Method for measuring dark current and multiplication gain

Evaluating the multiplication gain and the dark current is not straightforward with an 8 outputs EMCCD device like the CCD220. A very simple way to evaluate the mean multiplication gain is to use the measurement of the reset drain current. But this is again a global method, averaging the multiplication gain between the outputs although it is clear that a certain dispersion of gain is unavoidable with an 8 outputs EMCCD.

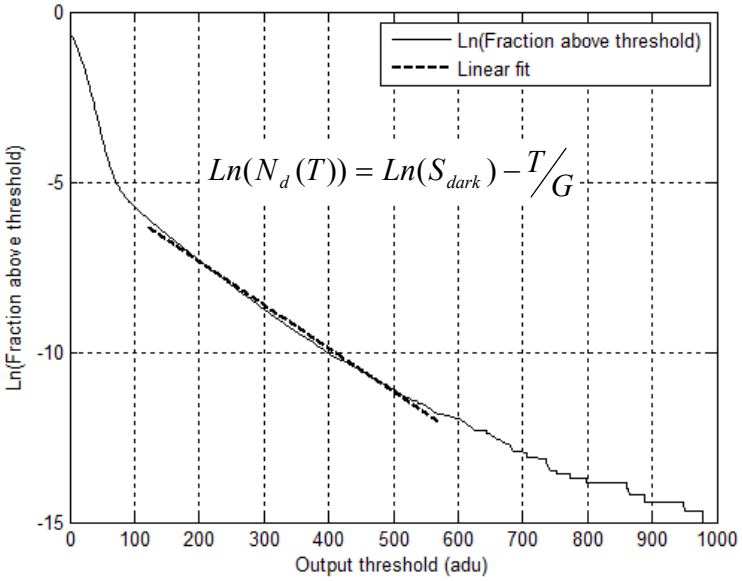

Figure 8. Method for computing dark signal and multiplication gain on the EMCCD when the camera is operated with multiplication gain. Statistics are obtained by combining all the pixels of a single output over 1000 consecutive frames (60x120 pixels, 1000 dark images). N_d is the fraction of pixels that are above a given threshold T, S_{dark} is the dark signal and G the multiplication gain. The dark signal and the multiplication gain can be determined by fitting a straight line to the linear part of this figure.

The way that dark current and the multiplication gain was determined for each output was based on an e2v technical note [18] for estimating ultra low level of dark signal in EMCCD devices. If the majority of dark signal is generated in the image/store section, then the dark signal level can be extracted from a simple analysis of the output distribution, even at very low signal levels.

For a certain threshold T of the pixel value, $N_d(T)$ is the fraction of pixels of the distribution that are above the threshold T, G is the multiplication gain and S_{dark} is the dark signal. $N_d(T)$, T, S_{dark} and G are linked by the following equation [18]:

$$Ln(N_d(T)) = Ln(S_{dark}) - T/G$$

This equation is only valid if the chance of getting two electrons in a pixel is insignificant. If it is not, i.e. if the dark signal is approximately greater than 0.1 electrons per pixel, then a more complex Monte Carlo analysis must be performed [18]. When this equation is valid, the plot of $Ln(N_d(T))$ as a function of the dark signal S_{dark} is linear. Measuring the slope of this linear plot and the intercept with the vertical axis, the dark signal S_{dark} and the multiplication gain G can be computed. The Figure 8 shows a typical plot obtained with OCam and the CCD220. The linear part of the plot is fitted in order to derive the dark signal and the multiplication gain. The plot was obtained by combining the 60x120 pixels of an output of 1000 consecutive dark images acquired at 1300 fps. This method has been validated by a large number of tests and by cross-comparison with the mean multiplication gain that is measured with the reset drain current ammeter. The method described has the advantage of separately measuring the multiplication gain for each output. The test is performed in complete darkness, thus reducing the possibility of damaging the detector from over-illumination while very high multiplication gains are applied.

To compute the noise with multiplication gain on the CCD, a set of 1000 consecutive dark images were recorded with multiplication gain of 1000 (~ 43-44V on high voltage clock).Then for each output, the histogram of all the 60x120 pixels over the 1000 images is plotted to have good statistics. The mean signal is subtracted to obtain centered histogram. RMS noise is computed by fitting the histogram with a Gaussian equation:

$$N(x) = A.e^{-x^2/2\sigma^2}$$

where σ is the measurement of the camera readout noise (in ADU).

The Figure 9 shows a typical noise histogram of OCam with multiplication gain (here 1570). Also shown on this figure is the Gaussian fit of the histogram:

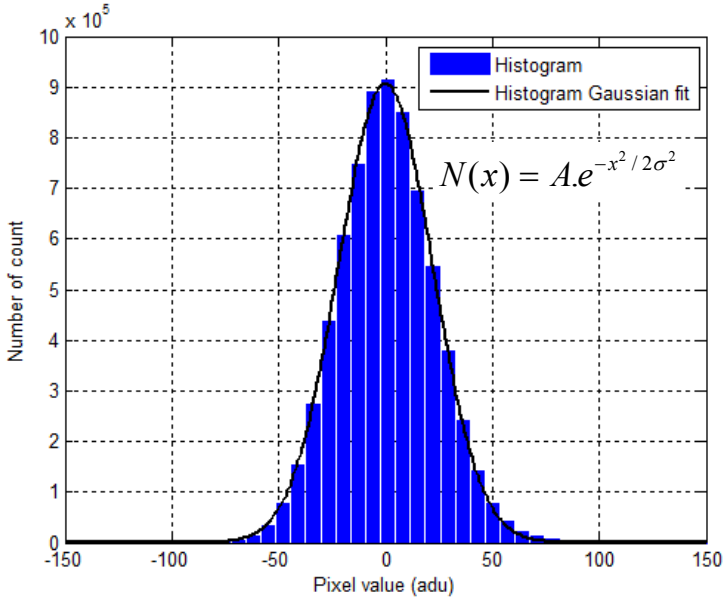

Figure 9. Method for computing readout noise with multiplication gain on the EMCCD. The signal is measured here includes the multiplication gain of the EMCCD (multiplication gain is here 1560). The σ parameter of the histogram Gaussian fit is the RMS noise of the camera.

From the Gaussian fit of the histogram, the RMS readout noise can be derived which is equal to the σ fitted value.

4.3 Dark, multiplication gain and noise measurement

Table 1 shows typical performances of the CCD220 tested with OCam. For the 8 outputs (Amp 0-7) of the CCD, the multiplication gain, the dark signal in e-/pixel/frame, the readout noise (using the "spatial" variance described in Figure 9) were measured. By multiplying the dark signal by the number of pixels of one output (60x120), the number of dark events per frame (in e-/frame) is calculated. The input referred noise (the readout noise at the input of the multiplication register) is calculated by dividing the output read out noise by the multiplication gain. Measurements presented here were performed at the detector temperature of -40°C, a frame rate of 1300 frames per second (fps) and a mean multiplication gain of 1380. Dark current was also measured at 25 fps with multiplication gain. Typical measured results are summarized in Table 2.

Table 1. Typical CCD220 and OCam measured performances at 1300 frames per second (fps) with a CCD temperature of -40°C. Sub-electron noise at 1300 fps was obtained for the first time. Mean dark signal is ~ 0.009 e/pixel/frame.

	HV Clock Voltage (V)	Multiplication Gain	Dark current (e-/pixel/frame)	Output Noise (e- rms)	Input Referred Noise (e- rms)	Dark Current (e-/frame)
Amp 0	43.5	1742	0.0093	870	0.50	67
Amp 1		1676	0.0094	486	0.29	68
Amp 2	43.4	1568	0.0084	439	0.28	60
Amp 3		1558	0.0089	698	0.45	64
Amp 4	44.9	1292	0.0088	994	0.77	63
Amp 5		1356	0.0066	443	0.33	48
Amp 6	43.9	956	0.0080	525	0.55	58
Amp 7		881	0.0097	864	0.98	70
Mean	**43.9**	**1379**	**0.0086**	**665**	**0.52**	**62**

The main measured results are:

- The mean read out noise input referred is ~0.52 e- at 1300 fps. The spread in readout noise of the 8 outputs is 0.28 e- to 0.98e-, in any case below 1 e-.
- The mean dark signal is ~0.009 e-/pixel/frame at 1300 fps, or ~62 e-/frame.

CCD220 and OCam is currently the only existing system to achieve such low noise performances at this high read out speeds. For the first time, sub-electron noise is reported with a frame rate of 1300 fps and a detector format of 240x240 pixels. This type of performance will open up a new era in the field of advanced wavefront sensing. For comparison, the NACO AO system currently in operation in Paranal on the ESO VLT uses the CCD50 detector from e2v and achieves 6-7e read noise at 500 Hz frame rate [19].

Figure 10 illustrates the typical noise behavior of an EMCCD. Left hand side of the figure concerns histograms with a unity gain while the right hand side of the figure shows histograms measured with multiplication gain. When the signal is multiplied, in this case by a factor of ~1570, the noise histogram is slightly broadened by a factor of 2 (see raw data in ADU, top part of the figure) but the input referred noise (in e-) is dramatically reduced from 205 to 0.32 e- (see bottom part of the figure).

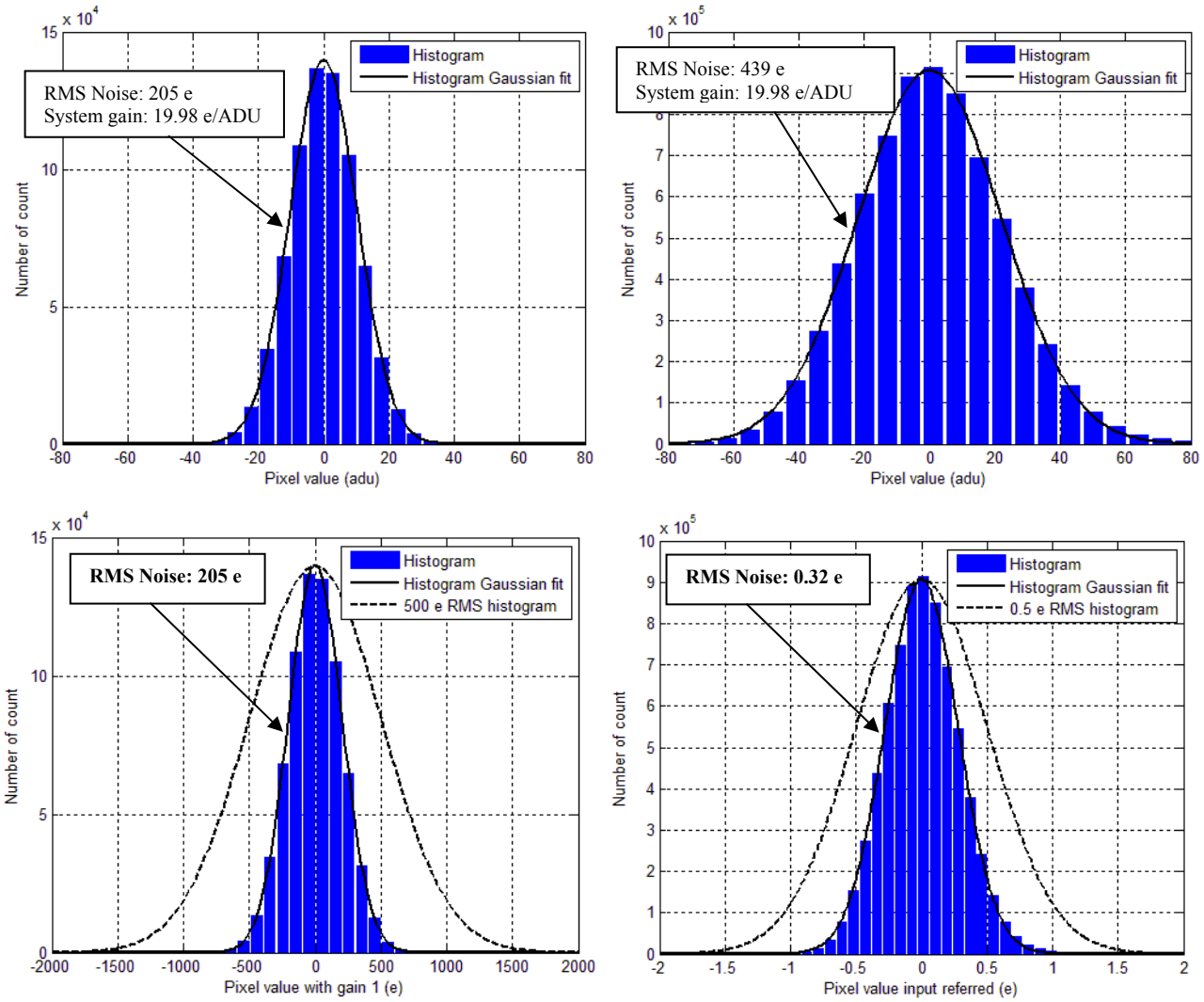

(a) Without multiplication gain (b) With multiplication gain of 1570

Figure 10: Noise histograms of output 2 of CCD220 with OCam. (a) Up left: Noise histogram without gain in ADU; Bottom left: Noise histogram without gain in e-. (b) Up right: Noise histogram with gain 1570 in ADU; Bottom right: Noise histogram with gain 1570 in e- and input referred. Noise as low as 0.32 e- RMS is measured here.

4.4 Quantum efficiency

The Quantum Efficiency (QE) of the detector is also a major parameter of the system sensitivity. The QE of the Standard Silicon CCD220 was measured and typical results are shown in Figure 11 using the calibration parameters of the previous section (i.e. a system gain of 20 e-/ADU). Also shown in this figure with square markers is the specified QE. It shows that the measured QE exceeds the specified value at all wavelengths and peaks at 94% at a wavelength of 650nm.

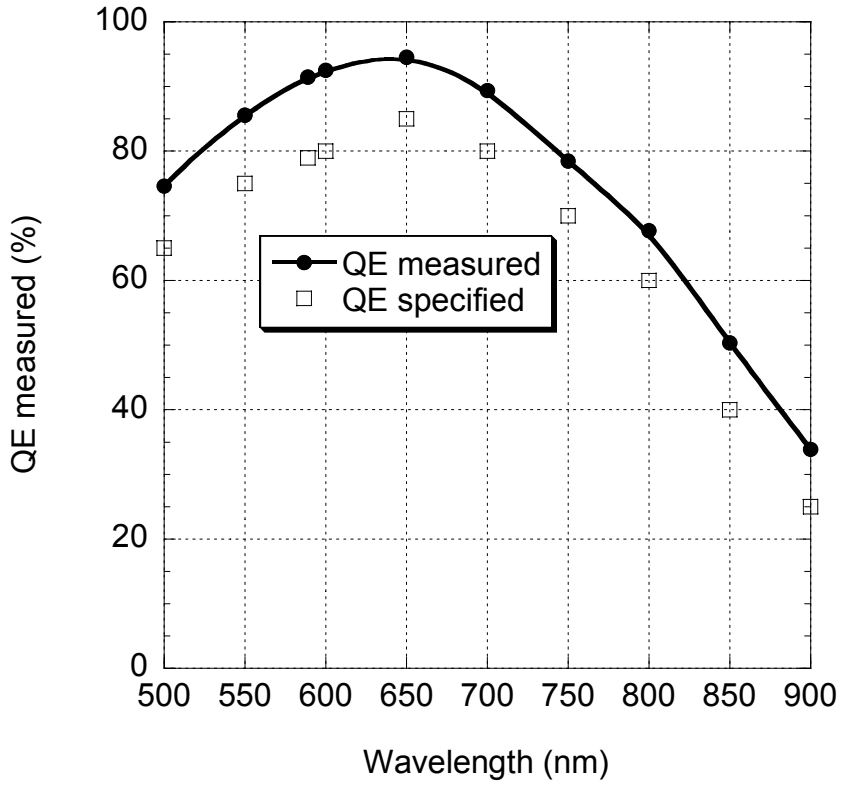

Figure 11. CCD220 measured Quantum Efficiency (QE) of standard Silicon variant compared to the specified values (square markers).

4.5 CCD220 and OCam performances measurement summary

Many other features of the CCD220 were tested with conventional methods that are not described here. These performances are summarized in Table 2. A first set of 4 electrical grades, 4 engineering grades and 4 science grades devices were first delivered as part of the original ESO/OPTICON contract in 2009. Since this milestone, production runs have started at e2v to routinely deliver CCD220 to customers.

Table 2. CCD220 and OCam measured performance summary

Test measurement	Result	Unit
Mean readout noise at 1300 fps	0.52	e
Dark signal at 1300 fps	0.01	e/pix/frame
Dark signal at 25 fps	0.05	e/pix/frame
Detector operating temperature	-40	°C
Peak Quantum Efficiency at 650 nm	94	%
Linearity at gain x1000 from 10 to 150 ke	<3	%
Image area Full Well Capacity at gain x1, 1300 fps	300	Ke-
Parallel CTE at gain x1, 1300 fps	>0.99995	N/A
Serial CTE at gain x1, 1300 fps	0.99994	N/A
Maximum Deviation from Peak to Valley over the light sensitive area	0.7	µm
Optical Distance from CCD image plane to front of window	3.33	mm
Angle between CCD image plane and front of window	0.11	degrees

5. ADVANCING FROM OCam TO OCam^2

OCam² is the production version of OCam. Whereas OCam has been designed to test CCDs and to have a lot of tuning capabilities (voltages, features and so-on), OCam² is a ready-to-use camera with embedded parameters to run the CCD, factory optimized. Apart from this, OCam^2 has been designed to be ruggedized and can accept more demanding environmental conditions, like a cooling water temperature up to 40°C making unnecessary a secondary external chiller. The camera is fully sealed, includes the Thermo Electric Cooler controller inside the camera head, and needs only a standard +24V power supply for the whole system. The OCam² camera is now a commercial product of First Light Imaging[4].

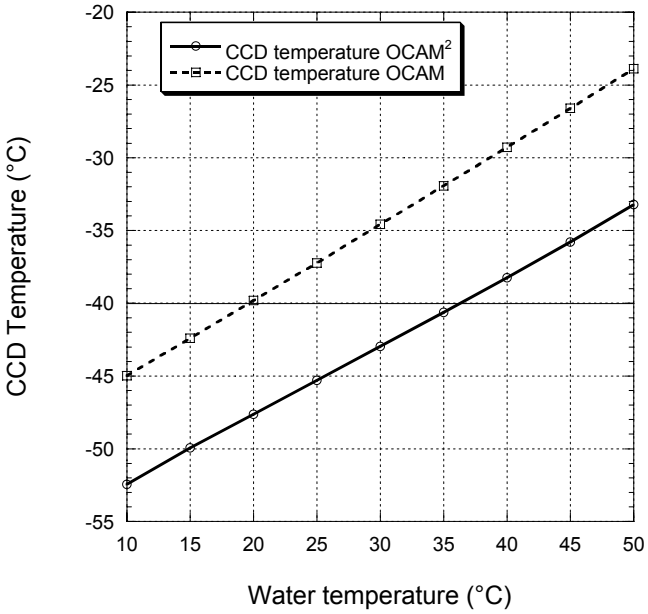

Figure 12. CCD temperature as a function of water temperature (flow of 1.5 l/min) used in the heat sink dedicated to cool down the Peltier hot side with outside air temperature of 30°C. As shown on this figure, OCam^2 can accommodate a water temperature as high as +40°C with a CCD temperature close to -40°C in these rugged conditions.

OCam² uses high performance FPGAs and can do instant on-the-fly pre-processing like dark / bias subtraction and flat-gain correction lowering the real time computer power that is required. OCam^2 provides not only an industry-standard CameraLink full interface but also duplex serial protocols over multimode or monomode optic fibers using standard SFP modules. Protocols like PCI Express, RapidIO and Infiniband are supported. Other specific or even proprietary fiber links can be implemented upon special request. Unique external synchronization and clock inputs of OCam^2 ensure a perfect synchronous operation of any number of OCam² at the nanosecond level. It is possible to synchronize OCam² with any external device (pulsed laser, another OCam² camera, master timer) with a precision of 10ns. OCam² includes also a modified mechanical design allowing integration of any type of microlens array for use of this camera in all kind of wavefront sensing AO applications. The front cover of OCam^2 can be easily modified to include a microlens exchange mechanism. The size of the camera head is extremely compact with a 238.5x175x76.2 mm footprint that includes all electronics, the CCD and the cooling system embedded in a robust aluminum sealed cover. The services needed to operate the camera are not demanding. OCam^2 only needs a 24V DC power supply and a water cooling system with the following typical specifications: a water flow of 1.5 l/min, a cooling power of 50W, and water temperature between 10 and 35°C.

With the capability of running at 2500 fps by using optimized clocking, a special preamplifier design that rejects clock feedthrough, and many other features, OCam^2 makes it an interesting contender for AO applications of the planned generation of Extremely Large Telescopes.

[4] First Light Imaging, http://www.firstlight.fr/.

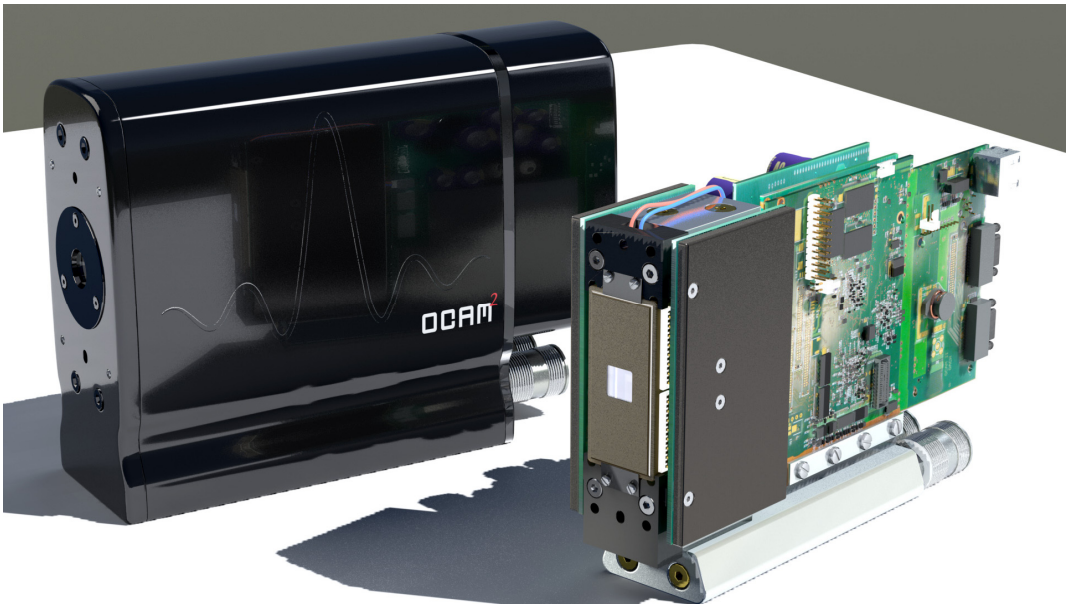

Figure 13. Picture of OCam^2; the OCam production camera commercialized by First Light Imaging. On the left hand side is shown the camera black aluminum cover. On the right hand side is shown the inside of the camera where the CCD220, all the electronic boards and the water heat exchanger can be seen.

6. CONCLUSION

For the first time, the CCD220 and OCam have demonstrated sub-electron noise for a 240x240 pixel camera system running at 1300 frames per second with the detector operated at a temperature of -40°C. This paper reports on the comprehensive, quantitative performance characterization of OCam and the CCD220 such as readout noise, dark current, multiplication gain, quantum efficiency, charge transfer efficiency. The CCD220 is a new detector fabricated by *e2v technologies* based on their L3Vision technology. It includes 8 outputs, split frame transfer architecture to lower detector smearing while the detector is read, 8 L3Vision registers to have multiplication gain and sub-electron noise at high speed. Both developed within the European OPTICON network [2], the CCD220 detector and the OCam camera were designed for AO applications with optimized performances in terms of noise and frame rate. A deep depleted variant of the CCD220 also exists with same overall performances and improved QE in the red.

A world record of 0.52 e mean RMS Noise was achieved with the 240x240 pixels CCD220 at 1300 frames per second. Under these conditions, the dark current is <0.01 e/pixel/frame and the peak QE is 94% at 650 nm wavelength due to back-thinning and back-illumination of the CCD. This achievement is a major breakthrough in the field of wavefront sensing for advanced Adaptive Optics systems to be used in the next generation of ground based telescope instruments.

A production camera, called OCam^2 and based on OCam experience, is designed and commercialized by First Light Imaging[5] to run at 1500 fps without degrading OCam performances. OCam^2 has been designed to be ruggedized and can accept more demanding environmental conditions. OCam^2 detector is fully cooled by 3 Peltier stages in order to avoid complex and costly cryogenic systems. Another advantage of this design is the extreme compactness of the camera head, embedding all the electronics (analogic, digital and Peltier drivers) that makes it easy to integrate into a multi-WFS AO system with an extremely small footprint. Ready to use, OCam^2 is designed for reliable operation on a telescope. Custom microlens array integration can easily be performed based on a flexible mechanical design of the front cover and past experience of microlens integration in the most advanced existing AO systems. A future development will start soon to speed up the frame rate of OCam^2 to 2500 Hz in order to accommodate the most demanding future AO applications.

[5] First Light Imaging, http://www.firstlight.fr/.

REFERENCES

[1] Moorwood, A., "Instrumentation at the ESO VLT ", Proc. SPIE 6269, 626904 (2006).

[2] Gillmore, G. F., "OPTICON: a (small) part of European astronomy", Proc. SPIE 5382, 138 (2004).

[3] Feautrier, P., Fusco, T., Downing, M., Hubin, N., Gach, J-L., Balard, P., Guillaume, C., Stadler, E., Boissin, O., Jorden, P., Diaz, J-J., "Zero noise wavefront sensor development within the Opticon European network", Scientific Detectors for Astronomy 2005, Springer Netherlands editor, ISBN: 978-1-4020-4329-1, Beletic, Jenna E.; Beletic, James W.; Amico, Paola (Eds.), Vol. 336 (2006).

[4] Jerram, P., Pool, P. J., Bell, R., Burt, D. J., Bowring, S., Spencer, S., Hazelwood, M., Moody, I., Catlett, N. and Heyes, P. S., "The LLCCD: low-light imaging without the need for an intensifier", in Proc. SPIE, 4306, pp. 178-186, May 2001.

[5] Fusco, T., Nicolle, M., Rousset, G., Michau, V., Beuzit, J-L, Mouillet, D., "Optimisation of Shack-Hartman based wavefront sensor for XAO systems", Advancements in Adaptive Optics. Edited by Domenico B. Calia, Brent L. Ellerbroek, and Roberto Ragazzoni. Proceedings of the SPIE, Volume 5490, pp. 1155-1166 (2004).

[6] Robbins, M., Hadven, B., "The Noise Performances of Electron Multiplying Charge-Coupled Devices", IEEE Transactions On Electron Devices, Vol. 50, No. 5, pp. 1227-1232 (2003).

[7] Petit, C., Fusco, T., Charton, J., Mouillet, D., Rabou, P., Buey, T., Rousset, G., Sauvage, J.-F. , Baudoz, P. , Gigan, P., Kasper, M., Fedrigo, E., Hubin, N., Feautrier, P. , Beuzit, J.-L., Puget, P. , "The SPHERE XAO system: design and performance", Proc. SPIE 7015, 70151D (2008).

[8] Beuzit, J., Feldt, M., Dohlen, K., Mouillet, D., Puget, P., Wildi, F., Abe, L., Antichi, J., Baruffolo, A., Baudoz, P., Boccaletti, A., Carbillet, M., Charton, J., Claudi, R., Downing, M., Fabron, C., Feautrier, P., Fedrigo, E., Fusco, T., Gach, J., Gratton, R., Henning, T., Hubin, N., Joos, F., Kasper, M., Langlois, M., Lenzen, R., Moutou, C., Pavlov, A., Petit, C., Pragt, J., Rabou, P., Rigal, F., Roelfsema, R., Rousset, G., Saisse, M., Schmid, H., Stadler, E., Thalmann, C., Turatto, M., Udry, S., Vakili, F., Waters, R., "SPHERE: a planet finder instrument for the VLT" in Ground-based and Airborne Instrumentation for Astronomy II, edited by Ian S. McLean, Mark M. Casali, Vol. 7014, 701418 (2008).

[9] Downing, M., Kolb, J., , Baade, D., Iwert, O., Hubin, N., Reyes, J., Feautrier, P., Gach, J-L., Balard, P., Guillaume, C., Stadler, E., Magnard, Y., "AO Wavefront Sensing Detector Developments at ESO", Proc. SPIE 7742-4, San Diego, (2010).

[10] Feautrier, P., Gach, J., Balard, P., Guillaume, C., Downing, M., Stadler, E., Magnard, Y., Denney, S., Suske, W., Jorden, P., Wheeler, P., Skegg, M., Pool, P., Bell, R., Burt, D., Reyes, J., Meyer, M., Hubin, N., Baade, D., Kasper, M., Arsenault, R., Fusco, T., Diaz Garcia, J. J., "The L3Vision CCD220 with its OCam test camera for AO applications in Europe" in High Energy, Optical, and Infrared Detectors for Astronomy III, edited by David A. Dorn, Andrew D. Holland, Proceedings of SPIE Vol. 7021, 70210C (2008).

[11] Downing, M., Finger, G., Baade, D., Hubin, N., Iwert, O., Kolb, J., "Detectors for AO wavefront sensing", Proc. SPIE 7015, 70151R (2008).

[12] Downing, M., Hubin, N., Kasper, M., Jorden, P., Pool, P., Denney, S., Suske, W., Burt, D. Wheeler, P., Hadfield, K., Feautrier, P., Gach, J-L, Reyes, J., Meyer, M., Baade, D., Balard, P. Guillaume, C., Stadler, E., Boissin, O., Fusco, T., Diaz, J-J., "A Dedicated L3Vision CCD for Adaptive Optics Applications", Scientific Detectors for Astronomy 2005, Springer Netherlands editor, ISBN: 978-1-4020-4329-1, Beletic, Jenna E.; Beletic, James W.; Amico, Paola (Eds.), Vol. 336 (2006).

[13] Downing, M., Arsenault, R., Baade, D., Balard, P., Bell, R., Burt, D., Denney, S., Feautrier, P., Fusco, T., Gach, J., Diaz Garcia, J. J., Guillaume, C., Hubin, N., Jorden, P., Kasper, M., Meyer, M., Pool, P., Reyes, J., Skegg, M., Stadler, E., Suske, W., Wheeler, P., "Custom CCD for adaptive optics applications" in *High Energy, Optical, and Infrared Detectors for Astronomy II*, edited by David A. Dorn, Andrew D. Holland, Proceedings of SPIE Vol. 6276, 62760H (2006).

[14] Feautrier, P., Stadler, E., Downing, M., Hurrell, S., Wheeler, P., Gach, J., Magnard, Y., Balard, P., Guillaume, C., Hubin, N., Diaz, J. J., Suske, W., Jorden, P., "Thermal modelling of cooled instrument: from the WIRCam IR camera to CCD Peltier cooled compact packages" in *Modeling, Systems Engineering, and Project Management for Astronomy II*, edited by Martin J. Cullum, George Z. Angeli, Proceedings of SPIE Vol. 6271, 62710S (2006).

[15] Reyes, J., Conzelman, R., "ESO AO Wavefront Sensor Camera", Detectors for Astronomy 2009 workshop, http://www.eso.org/sci/meetings/dfa2009/, ESO Garching, 12-16 October (2009).

[16] Gach, J-L., Balard, P., Boissin, O., Downing, M., Feautrier, P., Guillaume, C., Stadler, E. , "A dedicated controller for Adaptive Optics L3CCD developments", Scientific Detectors for Astronomy 2005, Springer Netherlands editor, ISBN: 978-1-4020-4329-1, Beletic, Jenna E.; Beletic, James W.; Amico, Paola (Eds.), Vol. 336 (2006).

[17] Janesick, J., [Photon transfer], SPIE Press Book, ISBN. 9780819467225, Vol. PM170, (2007).

[18] Robbins, M., "Estimating Ultra Low Levels of Dark Signal Using an L3Vision Device", e2v technical note, Doc. L3V-TN-635, http://www.e2v.com, (2005).

[19] Feautrier, P., Kern, P. Y., Dorn, R. J., Rousset, G., Rabou, P., Laurent, S., Lizon, J., Stadler, E., Magnard, Y., Rondeaux, O., Cochard, M., Rabaud, D., Delboulbe, A., Puget, P., Hubin, N. N., "NAOS visible wavefront sensor" in *Adaptive Optical Systems Technology*, edited by Peter L. Wizinowich, Proceedings of SPIE Vol. 4007, pp. 396-407 (2000).